Available online at www.sciencedirect.com
ScienceDirect
Ceramics International 33 (2007) 1325–1329
CERAMICS INTERNATIONAL
www.elsevier.com/locate/ceramint

Sintering behaviour of steatite materials with barium carbonate flux

E. Vela [a], M. Peiteado [b,*], F. García [a], A.C. Caballero [b], J.F. Fernández [b]

[a] Vicar S.A.C/ Rosas 3, 46940 Manises, Valencia, Spain
[b] Department of Electroceramics, Instituto de Cerámica y Vidrio, C/ Kelsen 5, 28049 Madrid, Spain

Received 9 March 2006; received in revised form 10 April 2006; accepted 24 April 2006
Available online 11 September 2006

Abstract

Steatite porcelains show excellent properties for insulating applications. New applications as small insulators for halogen bulbs lighting for instance, place increasing demands on material performance. The purpose of this work is to study the sintering behaviour and microstructural development of steatite ceramics formulated with $BaCO_3$ flux. Both constant heating rate and isothermal sintering experiments together with microstructure characterization have revealed important differences related to the presence of $BaCO_3$ and different amounts of clay. Increasing the amount of clay leads to higher vitreous/crystalline phase ratios but also to smaller grain sizes. This result is interesting because of the relevant role played by the grain size for the protoenstatite to clinoenstatite transformation, which in turns is the origin of material aging and degradation.

Keywords: A. Sintering; B. Microstructure-final; B. Grain size; D. Porcelain

1. Introduction

Traditionally porcelains are ceramic materials used for manufacturing insulator devices [1,2]. Two main families can be distinguished in the porcelain compositions: on one hand triaxial porcelains made of kaolin and/or clay, feldspar and quartz or alumina and on the other hand steatite porcelains based on talc, clay and auxiliary fluxes such as feldspar or barium carbonate. General microstructure of porcelains is mainly composed of crystalline particles surrounded by a vitreous phase and a certain amount of pores [3–5]. This vitreous phase controls the sintering process and has a great influence on the mechanical and dielectric properties of the material [6]. Because of the increasing interest in triaxial porcelains for manufacturing porcelain stoneware tiles, recent works have been reported dealing with their microstructure development and the sintering behaviour [7–10]. However for electrical insulating applications, the best dielectric properties are shown by steatite porcelains, also known simply as steatites. Their optimum dielectric properties are resumed in the norm CEI 672-1 of the CENELEC (European Committe for Electrotechnical Standarization) in the steatite group C221 [11].

Steatites are based on the generation of a crystalline phase of magnesium metasilicate from talc mineral according to the following reaction:

$$3MgO \cdot 4SiO_2 \cdot H_2O \xrightarrow{\Delta T} 3MgSiO_3 + SiO_2 + H_2O \quad (1)$$

Talc is agglomerated with clay, and some fluxes as feldspar or barium carbonate are added for generating enough vitreous phase. Whenever the auxiliary flux is a feldesphatic material, alkaline ions lead to a low performance steatite with increased dielectric losses (classified as much as C220); on the contrary, if the flux is barium carbonate, the dielectric properties of steatite are optimum [12,13]. Nevertheless in both cases the sintering of the ceramic takes place in the presence of a liquid phase and as previously mentioned, the microstructure after cooling is composed by crystalline magnesium metasilicate grains surrounded by a vitreous matrix. Among the three possible magnesium metasilicate polymorphs, protoenstatite, ortoenstatite and clinoenstatite [14–16], the first one is thermodynamically stable at high temperature (until 985 °C) but is the main crystalline phase in steatite porcelains because it is stabilized by the vitreous phase; the average size of protoenstatite crystals stays normally below 10 μm. However if protoenstatite crystals are not properly stabilized, transformation to the room

* Corresponding author at: Advanced Materials Department, Jozef Stefan Institute, Jamova 39, 1000 Ljubljana, Slovenia. Tel.: +386 1 4773629; fax: +386 1 4773875.
E-mail address: marco.peiteado@ijs.si (M. Peiteado).

0272-8842/$32.00
doi:10.1016/j.ceramint.2006.04.015

temperature polymorph, clinoenstatite, will occur [17] and this martensitic type of transformation implies a volume change that leads to extensive material cracking. For years, this has been the origin of material damage during manufacturing and service [18,19].

Although interest on these materials is increasing in the last years because of their application in new fields, such as that of small insulators for halogen bulbs lighting, few work has been developed dealing with the sintering behaviour as well as the microstructure evolution of these porcelains. Moreover, understanding microstructural development becomes a critical point to design steatite materials that satisfy the increasing demands on the material performance required by the new applications. In this way the present work is focused on the study of the sintering process in steatite materials in order to understand and control their microstructure development.

2. Experimental procedure

A family of compositions in the SiO_2–Al_2O_3–MgO system were prepared to follow the sintering behaviour in steatite porcelains (Table 1). These compositions labelled TA1–TA5 were designed increasing both the Al_2O_3 content, which shifts the composition towards the eutectic point of the system, as well as the SiO_2/MgO ratio. Talc, clay and barium carbonate were used as raw materials. X-ray diffraction pattern in Fig. 1a shows that the starting talc mineral presented a high purity level with minor amounts of dolomite and clorite phases. Clay was mainly kaolinitic with minor quantities of quartz and illite (Fig. 1b) and barium carbonate was 99.7% pure. Compositions were prepared by wet milling of raw materials in a jar mill. After milling (90% of the particles <25 μm) pressing additives were added and the slurries were homogenized for 1 h. The slips were then passed through a 325 mesh sieve and rheological parameters were adjusted for spray-drying in a Niro spray-drier with rotating disc. Discs of 60 mm diameter were uniaxially pressed at 40 MPa and less than 0.5% humidity. After drying at 110 °C for 24 h, the pressed discs were fired at 5 °C/min heating rate and 60 min soaking time at maximum temperature which ranged from 1240 to 1380 °C.

Characterization of raw materials was performed by X-ray diffraction (XRD) on a D5000 Siemens diffractometer with a fully computerized Kristalloflex 710 generator using Cu $K\alpha_1$ radiation and Ni filter. Dilatometric measurements were performed in air at a 5 °C/min heating rate on a Netzch 407/E Dilatometer. Microstructural observations with scanning electron microscopy (SEM) were carried out on both polished and fracture surfaces of selected samples in a Field Emission Hitachi S-4700 FE-SEM microscope. Grain/pore size measurements (including distribution of phases) were evaluated from SEM micrographs of polished and chemically etched samples by an image processing and analysis program (Leyca) that measures the surface of each grain and transforms its irregularly shaped area into a circle of equivalent diameter. More than 400 grains/pores were considered for each measurement.

Table 1
Molar relations of compositions prepared to follow the sintering behaviour in steatite porcelains

	TA1	TA2	TA3	TA4	TA5
SiO_2	1.00	1.00	1.00	1.00	1.00
MgO	0.76	0.74	0.72	0.70	0.68
Al_2O_3	0.02	0.03	0.04	0.05	0.06
BaO	0.03	0.03	0.03	0.03	0.03
SiO_2/MgO	1.32	1.35	1.39	1.13	1.18

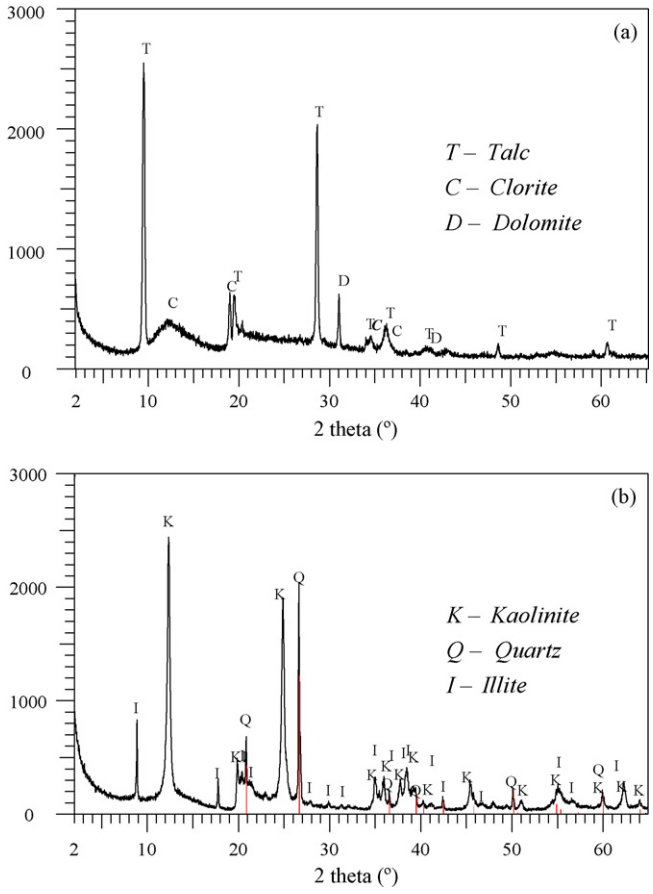

Fig. 1. XRD patterns of the raw-materials: (a) talc and (b) clay.

3. Results and discussion

Fig. 2 depicts the shrinkage and shrinkage rate evolution with temperature for samples of TA1 and TA5 compositions. As observed shrinkage starts around 800 °C in both compositions but increases with the clay content at the initial sintering stage. Looking into shrinkage rate curves (Fig. 2b) two peaks can be observed in the range between 800 and 1000 °C; the first one appearing at lower temperature is related to $BaCO_3$ decarbonation and the second one, which also increases with the clay content, is related to dehidroxilation of the talc mineral introduced in the compositions and metakaolin transformation originated from the clay mineral. Hence, below 1000 °C sample shrinkage is attributed to changes of raw materials with no apparent reactions between them. Around this temperature the $BaCO_3$ decarbonation is already finished and submicronic

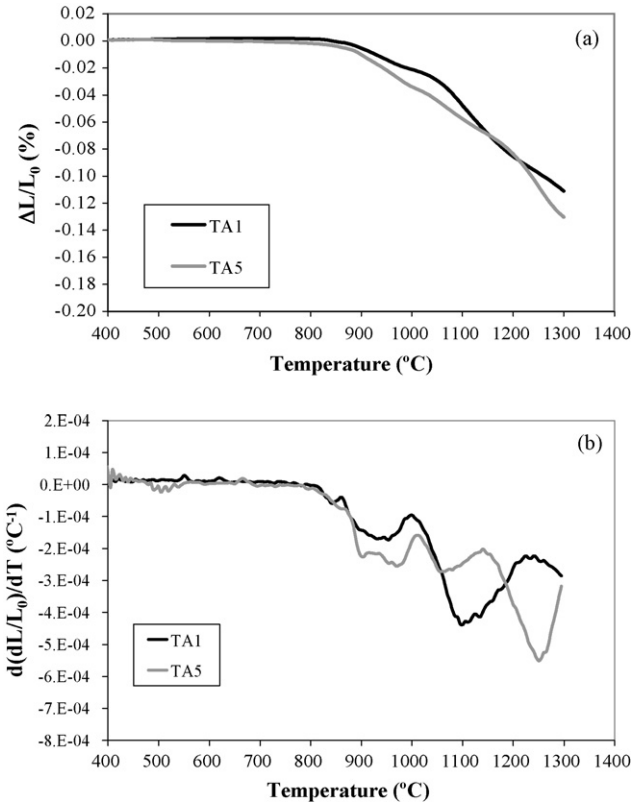

Fig. 2. Shrinkage (a) and shrinkage rate (b) behaviour of compositions TA1 and TA5.

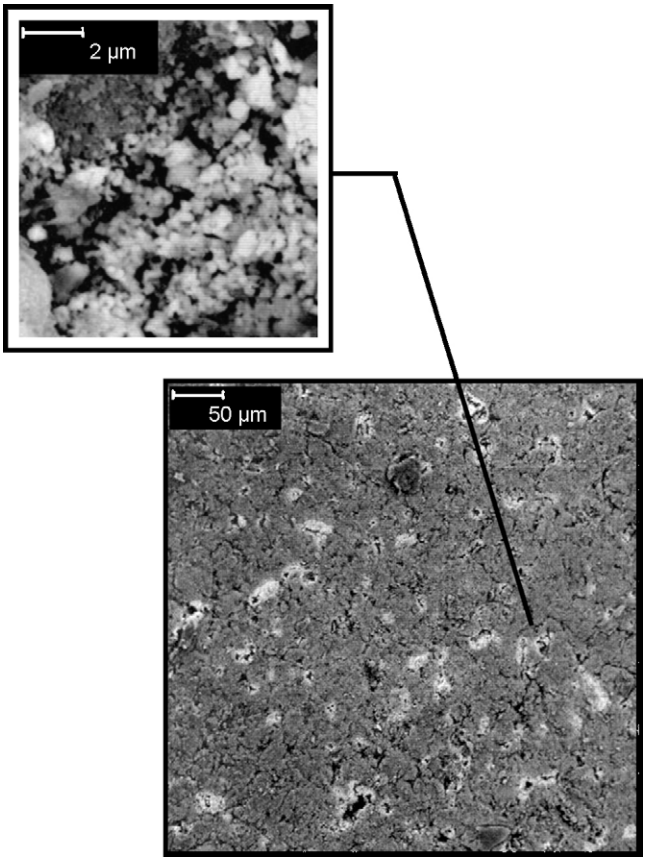

Fig. 3. Detail of BaO particles formed in composition TA1 fired at 1000 °C as a result of $BaCO_3$ decarbonation (SEM micrograph of polished sample).

agglomerates of barium oxide can now be observed (Fig. 3). These highly reactive particles start to react then with amorphous metakaolinite coming from clay kaolinite as well as with silica coming from talc. In fact the temperature of this reaction (around 1000 °C) is markedly lower than the eutectic temperature (1122 °C) probably due to the high reactivity of nanometric size barium oxide particles [20–23]. As a consequence, a small amount of liquid phase starts to appear where $BaCO_3$ particles were lying. Taking into account that the eutectic composition is roughly 27% BaO, 60% SiO_2 and 13% Al_2O_3 (in mol%) and BaO content is 4.2% for all compositions, the complete reaction of BaO requires a 9.3% of SiO_2 and 2% of Al_2O_3 to be consumed. This means that only in TA5 composition there is enough metakaolinite to supply the necessary SiO_2, whereas in TA1 composition BaO particles should react mainly with silica coming from the talc transformation to protoenstatite according to reaction (1). The less silica coming from clay, the more will be incorporated from the excess of dehidroxilated talc; however, this last source of silica is less reactive than that one coming from decomposition of clay minerals. Consequently, shrinkage behaviour is very different for both samples above 1000 °C (Fig. 2). For TA5 composition the formation of the liquid phase seems to be completed between 1050 and 1150 °C and the densification rate is higher than that of TA1 composition where

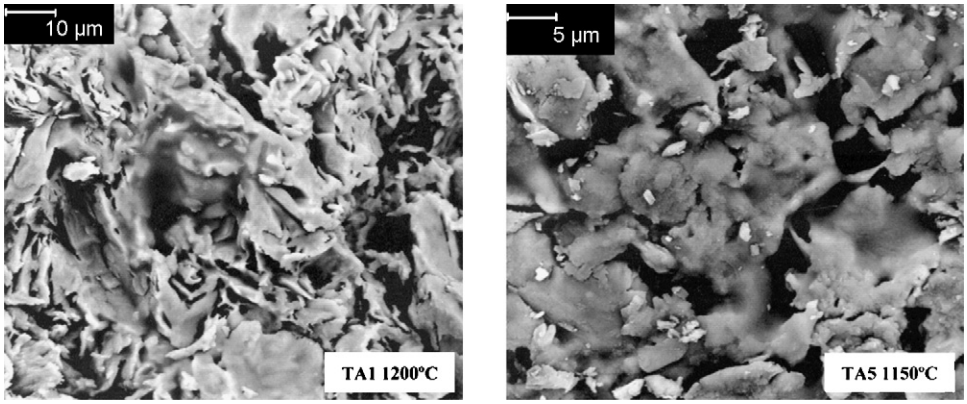

Fig. 4. Evidence of liquid phase in the microstructure of samples of TA1 and TA5 compositions after sintering at 1200 and 1150 °C, respectively.

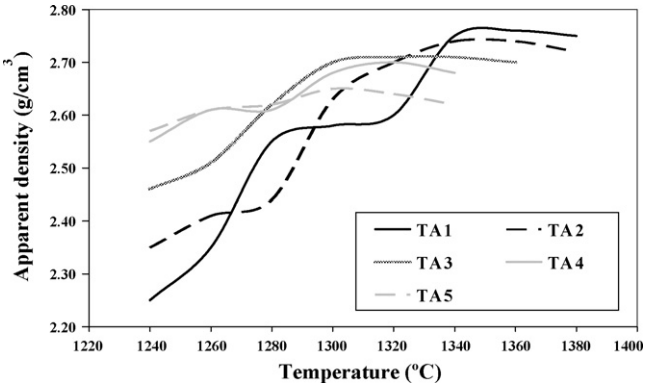

Fig. 5. Densification of TA compositions as a function of sintering temperature.

the same process is extended up to 1250 °C. Such a different behaviour is reflected in the microstructure evolution of both systems: as inferred from SEM micrographs (Fig. 4) the evidence of liquid phase is more generalized in sample of TA5 composition treated at 1150 °C than in sample of TA1 composition treated at 1200 °C.

In the same way Fig. 5 plots the density of the sintered samples versus temperature for isothermal sintering experiments. A general behaviour is clearly observed. For lower sintering temperatures (below 1300 °C) the density of the sintered pellets increases with the clay content. On the contrary, this trend reverses for sintering temperatures approaching 1350 °C. Furthermore a lowering of the maximum apparent density is observed from TA1 to TA5 compositions (Fig. 5). This fact should be interpreted considering that the main factor affecting these samples is the vitreous/crystalline phase relation: the higher the amount of vitreous phase (higher vitreous/crystalline phase relation) the lower the maximum apparent density. Data in Table 2, corresponding to samples of each composition sintered at their maximum density, clearly shows that such relation increases from TA1 to TA5. Besides, the microstructural analysis of these samples sintered at their maximum density reveals two main differences between compositions, related to the distribution of phases as well as to the grain size of the crystalline phase (Fig. 6). On one hand the analysis of pore distribution shows that average pore size increases with alumina content, that is small pores in TA1 composition grow

Table 2
Microstructural characterization of compositions TA1–TA5. Samples sintered at the temperature of maximum density (see also Fig. 5)

	Maximum sintering density (g/cm^3)	Average grain size (+0.5 μm)	Average pore size (+0.5 μm)	Vitreous phase (%)
TA1	2.76	3.9	6.7	34
TA2	2.74	3.1	9.4	33
TA3	2.71	2.2	11.8	52
TA4	2.70	1.9	11.0	57
TA5	2.65	1.7	12.4	60

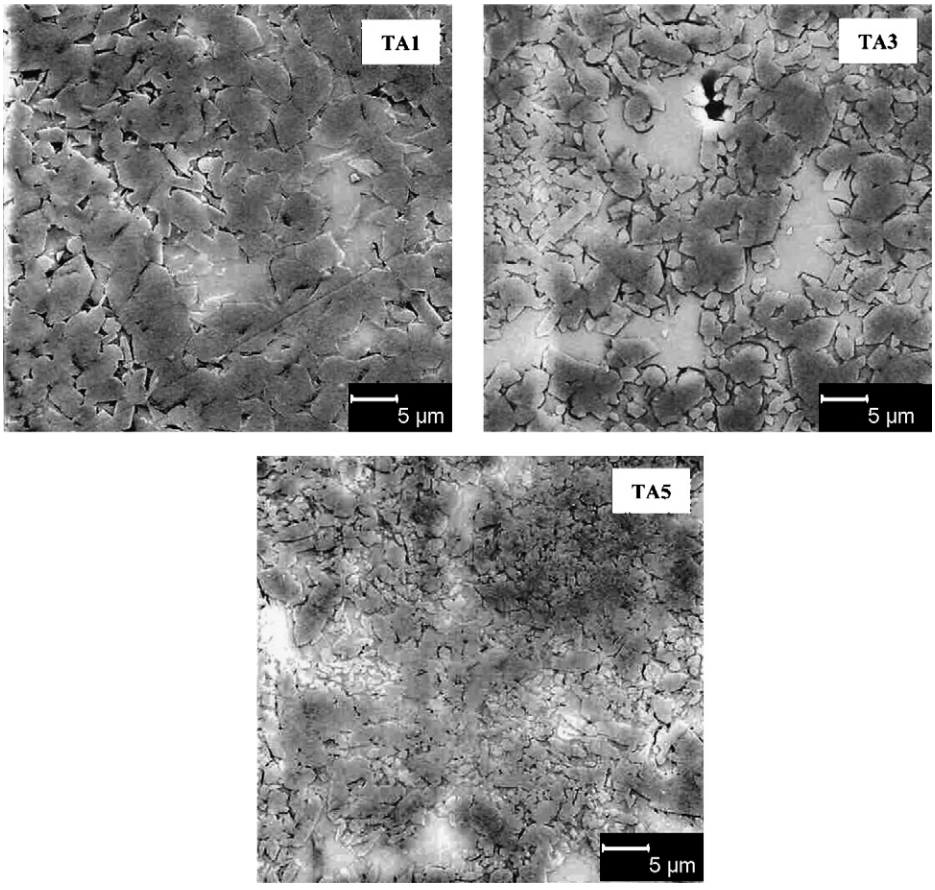

Fig. 6. Microstructure of TA compositions sintered at their temperature of maximum density, 1360 °C for TA1 composition, 1320 °C for TA2 and 1300 °C for TA3.

towards wider distributions in the other compositions (see Table 2). This seems to be related to mechanisms of pores coalescence associated with an increasing amount of low viscosity liquid phase that might lead to large pores quite difficult to be removed. On the other hand grain size measurements of the crystalline phase show the opposite trend with a decreasing average grain size when increasing alumina content (from TA1 to TA5, Table 2). Note that decreasing crystalline phase grain size is an important issue for material stability since large grains seem to show a strong trend to transform from protoenstatite to clinoenstatite. Moreover, this last result is rather surprising since the total amount of liquid phase increases with the alumina content (Table 2). To understand this, we should look it from the point of view of the liquid phase evolution at each composition. In all cases a first liquid phase is generated at low temperatures due to BaO formation from starting barium carbonate. This first liquid leads to a primary rearrangement which is more effective for the samples containing more clay. When temperature increases and alumina content is higher in the composition, the liquid phase, originated from the reaction between silica, magnesia and alumina, becomes more important and penetrates the dehidroxilated talc particles breaking them and leading to a secondary rearrangement. This process takes place at high temperatures and can explain why average crystal size lowers in the more fluxing compositions.

4. Conclusions

The sintering behaviour in steatite porcelains is mainly controlled by the reaction that takes place between BaO coming from $BaCO_3$ decarbonation in one hand, and amorphous metakaolinite coming from clay kaolinite and silica coming from talc in the other hand. Silica coming from clay is more reactive than the one coming from the silica excess of dehidroxilated talc, therefore increasing the amount of metakaolinite improves the liquid phase formation and shrinkage rate at low temperatures. When the sintering temperature increases and the alumina content is higher according to the amount of clay incorporated, the liquid phase originated from the reaction between silica, magnesia and alumina penetrates the dehidroxilated talc particles leading to a secondary rearrangement. This process leads to a decrease of the average grain size of the crystalline phase in spite of the increase of the vitreous/crystalline phase ratio. This is expected to improve the aging behaviour of the material since large grains seem to show a strong trend to transform from protoenstatite to clinoenstatite.

Acknowledgment

This work has been conducted within the CICYT MAT2004-04843-C02-01 project.

References

[1] W.M. Carty, U. Senapati, Porcelain: raw materials, phase evolution and mechanical behaviour, J. Am. Ceram. Soc. 81 (1) (1998) 3–20.
[2] J. Liebermann, Microstructure, properties and product quality of strength-stressed high voltage insulators, Am. Ceram. Soc. Bull. 82 (2) (2003) 39–46.
[3] Y. Iqbal, W.E. Lee, Fired porcelain microstructure revisited, J. Am. Ceram. Soc. 82 (12) (1999) 3584–3590.
[4] W.M. Carty, Observations on the glass phase composition in porcelains, Ceram. Eng. Sci. Proc. 23 (2) (2002) 79–94.
[5] L. Sanchez-Munoz, S.da.S. Cava, C.A. Paskocimas, Modelling of the vitrification process of ceramic bodies for whiteware, Ceramica 48 (308) (2002) 217–222.
[6] P. Ctibor, J. Sedlacek, K. Neufuss, J. Dubsky, P. Chraska, Dielectric properties of plasma-sprayed silicates, Ceram. Int. 31 (2) (2005) 315–321.
[7] R.D. Gennaro, P. Cappelletti, G. Cerri, M. de Gennaro, M. Dondi, G. Guarini, A. Langella, D. Naimo, Influence of zeolites on the sintering and technological properties of porcelain stoneware tiles, J. Eur. Ceram. Soc. 23 (13) (2003) 2237–2245.
[8] P.M.T. Cavalcante, M. Dondi, G. Ercolani, G. Guarini, C. Melandri, M. Raimondo, E.R. Rocha e Almendra, The influence of microstructure on the performance of white porcelain stoneware, Ceram. Int. 30 (6) (2004) 953–963.
[9] G. Bolelli, V. Cannillo, L. Lusvarghi, T. Manfredini, C. Siligardi, C. Bartuli, A. Loreto, T. Valente, Plasma-sprayed glass–ceramic coatings on ceramic tiles: microstructure, chemical resistance and mechanical properties, J. Eur. Ceram. Soc. 25 (11) (2005) 1835–1853.
[10] L. Esposito, A. Salem, A. Tucci, A. Gualtieri, S.H. Jazayeri, The use of nepheline-syenite in a body mix porcelain stoneware tiles, Ceram. Int. 31 (2) (2005) 223–240.
[11] CEI 672 Norm, Part 1: specifications for ceramic and glass insulating materials, Definitions Classif. (1995).
[12] M.D. Rigterink, Microscopic and X-ray investigation of some steatite bodies, J. Am. Ceram. Soc. 30 (7) (1947) 214–218.
[13] H. Thurnauer, A.R. Rodriguez, Notes on the constitution of steatite, J. Am. Ceram. Soc. 25 (15) (1942) 443–445.
[14] W.L. Brown, J.V. Smith, High temperature X-ray studies on the polymorphism of $MgSiO_3$, Z. Kristallogr. 118 (1963) 186–212.
[15] W.E. Lee, A.H. Heuer, On the polymorphism of enstatite, J. Am. Ceram. Soc. 70 (5) (1987) 349–360.
[16] C.M. Huang, D.H. Kuo, Y.J. Kim, W.M. Kriven, Phase stability of chemically derived enstatite ($MgSiO_3$) powders, J. Am. Ceram. Soc. 77 (101) (1994) 2625–2631.
[17] W. Mielcarek, D. Nowak-Wozny, K. Prociow, Correlation between $MgSiO_3$ phases and mechanical durability of steatite ceramics, J. Eur. Ceram. Soc. 24 (15/16) (2004) 3817–3821.
[18] V.I. Vereshchagin, V.N. Gurina, Polymorphism of magnesium metasilicate and its role in the production of no aging steatite ceramics, Glass Ceram. 54 (11/12) (1997) 365–367.
[19] X. Peicang, Z. Xiayoun, Mineral physical characteristics of pyroxene phase transformation and a probe into the mechanism of talc porcelain aging, Acta Mineral. Sin. 8 (2) (1988) 104–112.
[20] A.C. Caballero, J.F. Fernandez, M. Villegas, C. Moure, P. Duran, P. Florian, J.P. Coutures, Intermediate phase development in phosphorous doped barium titanate, J. Am. Ceram. Soc. 83 (6) (2000) 1499–1505.
[21] W.A. Jesse, G.J. Shiflet, G.L. Allen, Equilibrium phase diagram of isolated nanophases, Mater. Res. Innovat. 2 (1999) 211–216.
[22] R. Vallee, M. Wautelet, J.P. Dauchot, M. Hecq, Size and segregation effects on the phase diagrams of nanoparticles of binary systems, Nanotechnology 12 (1) (2001) 68–74.
[23] M. Wautelet, J.P. Dauchot, M. Hecq, Size effects on the phase diagrams of nanoparticles of various shapes, Mater. Sci. Eng. C 3 (1/2) (2003) 187–190.